

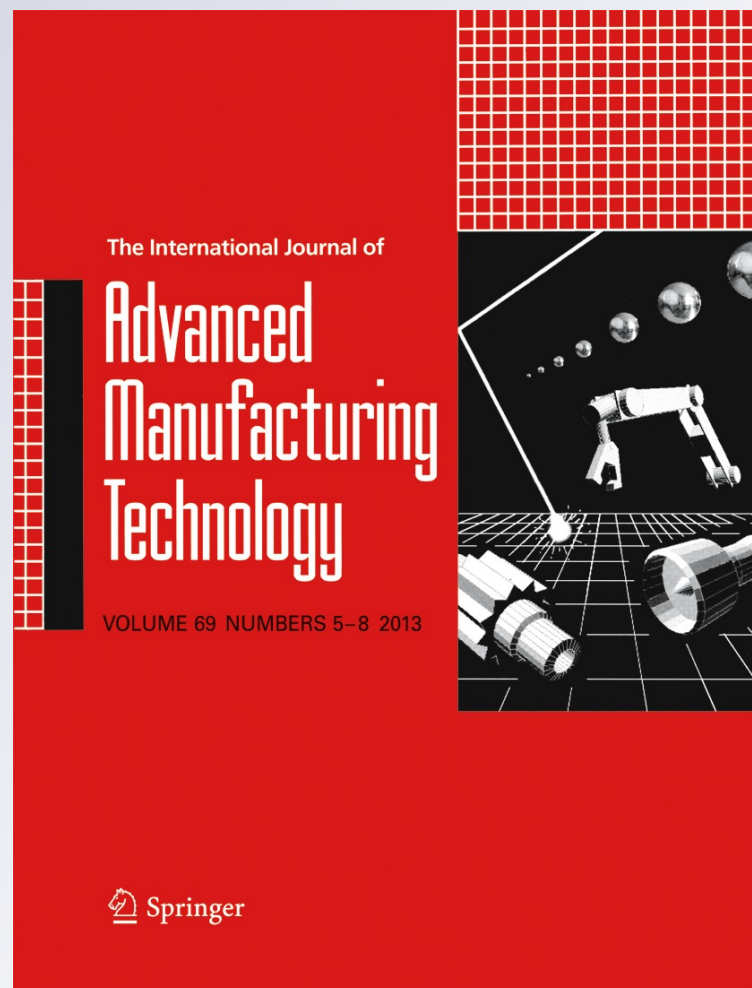
Effect of gap on plasma and molten pool dynamics during laser lap welding for T-joints

**Wei Meng, Zhuguo Li, Jian Huang,
Yixiong Wu & Rui Cao**

**The International Journal of
Advanced Manufacturing Technology**

ISSN 0268-3768
Volume 69
Combined 5-8

Int J Adv Manuf Technol (2013)
69:1105-1112
DOI 10.1007/s00170-013-5095-6



Your article is protected by copyright and all rights are held exclusively by Springer-Verlag London. This e-offprint is for personal use only and shall not be self-archived in electronic repositories. If you wish to self-archive your article, please use the accepted manuscript version for posting on your own website. You may further deposit the accepted manuscript version in any repository, provided it is only made publicly available 12 months after official publication or later and provided acknowledgement is given to the original source of publication and a link is inserted to the published article on Springer's website. The link must be accompanied by the following text: "The final publication is available at link.springer.com".

Effect of gap on plasma and molten pool dynamics during laser lap welding for T-joints

Wei Meng · Zhuguo Li · Jian Huang · Yixiong Wu · Rui Cao

Received: 2 January 2013 / Accepted: 27 May 2013 / Published online: 12 June 2013
© Springer-Verlag London 2013

Abstract The aim of the present research is to discuss the effect of gap on plasma plume, keyhole, and molten pool dynamics during laser lap welding for T-joints. The authors observe plasma plume, keyhole opening, and molten pool images by high-speed camera in different gaps during CO₂ laser overlap welding of T-joints. The results show that gap causes beam energy fluctuations in the keyhole and leads to the instability of welding process. In laser spot welding, zero-gap and small gap greatly affect the stability of plasma and keyhole, which causes the formation of cavities in the weld metal, while a proper gap can help prevent porosity formation. In laser continuous welding, the disruption and closure of front keyhole wall at the gap periodically changes with the gap, which causes the formation of plenty of porosities at the gap. The instability of keyhole is closely related to dynamics of plume and molten pool, which gives an insight into the mechanism of porosity formation during laser overlap welding.

Keywords Laser lap welding · Plasma plume · Molten pool · Gap · Instability · Porosity

1 Introduction

Laser lap welding can be divided into two kinds of types: laminated lap welding and stake lap welding. Stake welded T-joint is the simplest structural unit of all metal sandwich structures as shown in Fig. 1, in which the core and cover plates are bonded by laser welding. In order to reduce the gap between the core and cover sections, the core plates must be fabricated to maintain linearity along the length and proper height, while the gap induced by the fixing force and welding distortion is unavoidable during laser welding [1]. Up to now, the influence of gap on welding process is still not clear, particularly the dynamics of keyhole and molten pool in different gaps.

The dynamics study of plasma plume, keyhole, and molten pool in laser welding is essential to understand the welding process and the appearance of weld defects. Dynamics of plasma and keyhole in deep penetration welding has been studied by some experiments and numerical simulations [2–5]. Poueyo-Verwaerde et al. [6] and Szymanski and Kurzyna [7] applied spectroscopic measurements and diagnostics to observe the plasma induced in laser welding process. The results indicated that the plasma greatly affected the energy transmission during laser welding. Matsunawa et al. [8] observed keyhole behavior in continuous-wave and pulsed laser welding by using a similar x-ray transmission imaging system and found porosity is formed from bubbles generated from the tip of the keyhole. Seto et al. [9] observed the keyhole and the plasma plume behavior by high-speed camera and X-ray transmission imaging system, and found that the keyhole depth was closely related with the change of plume. Guohua Li et al. [10] acquired the stability information from plasma images taken

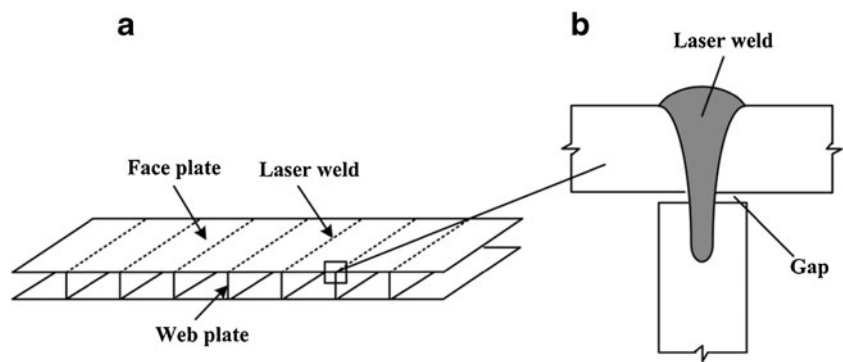
Research highlights: • Plasma and molten pool dynamics in different gap sizes were observed.

W. Meng · Z. Li (✉) · J. Huang · Y. Wu
Shanghai Key Laboratory of Material Laser
Processing and Modification, School of Materials
Science and Engineering, Shanghai Jiao Tong
University, Shanghai 200240, China
e-mail: lizg@sjtu.edu.cn

Y. Wu
State Key Laboratory of Metal Matrix Composites,
School of Materials Science and Engineering,
Shanghai Jiao Tong University,
Shanghai 200240, China

R. Cao
State Key Laboratory of Gansu Advanced
Non-Ferrous Metal Materials, Lanzhou University
of Technology, Lanzhou 730050, China

Fig. 1 Construction of web–core sandwich: **a** laser-welded all-metal sandwich panel and **b** laser-welded overlap T-joint



by high-speed photography and analyzed the influences of surface impurity and the flow rate of side-assist gas on the stability. Hiroshi et al. [11] observed dynamics of keyhole during laser penetration welding by using an X-ray transmission imaging system and found that the upper part of the keyhole fluctuated largely. Many bubbles in the molten pool were trapped by the solidifying wall, resulting in the porosity.

However, few studies have been conducted to reveal the relationship between the dynamics of plasma and keyhole during laser overlap welding, particularly the effect of gap in lap welding. In this study, we observed plume images, keyhole, and molten pool images simultaneously by using two high-speed cameras in CO₂ laser overlap welding for T-joints. The effect of gap on plasma plume, keyhole, and molten pool dynamics and porosity during laser lap welding for T-joints was revealed and discussed.

2 Experimental procedures

High-strength low alloy (HSLA) steel with 4 mm in thickness was used as a specimen in this experiment. The experimental setup is shown in Fig. 2. Overlap welding was carried out with the 15 kW CO₂ laser system. The laser beam was focused on the upper plate surface with a parabolic mirror of 357 mm focal length. The M2 value of the laser

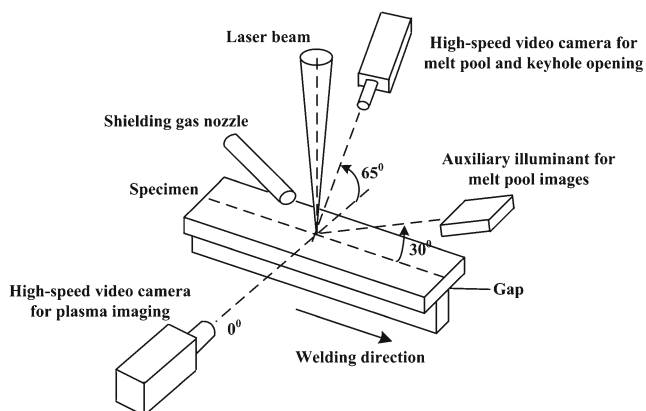


Fig. 2 Schematic illustration of the experimental setup

beam was about 3.6 and the spot diameter was 0.86 mm. Helium shielding gas was blown forward through a nozzle of a 6 mm internal diameter at a flow rate of 30 L/min. The welding speed was 1.5 m/min.

Dynamic behavior of the keyhole, molten pool, and plasma plume was simultaneously observed by the methods described in Fig. 2 in both laser spot welding and laser continuous welding. A high-speed camera system (HSCS) including high-speed camera, macro lens, dimmer glass, interference filter, and UV lens was used. The camera produced in Switzerland was MV-D1024-TrackCam of Photonfocus Company. Laser-induced plume and molten pool were observed by using high-speed camera placed in the horizontal plane and in the 65° dip angle, respectively. The flaming rate of the video was set as 1,000 frames per second for the plume and 750 frames per second for molten pool. The molten pool was illuminated with a diode laser (2 W at a wave length 808 nm) from horizontal plane with a 30° dip angle.

3 Results

3.1 Dynamics of plasma and molten pool in laser spot welding in different gap sizes

Dynamics of plume were observed by high-speed video cameras in laser spot welding of T-joints in different gap sizes. Figure 3 shows the flaming images of the laser-induced plume during laser spot welding in different gap sizes. As shown in Fig. 3, the plume began to emerge after 1.5 ms when a conduction welding was progressing. Plasma plume generated violently from the upper surface after about 3 ms. At this time, the recoil force of metal vapor became larger, leading to a large amount of plasma spurting [12]. The laser beam penetrated upper plate after 21.7 ms, when a small round plume could be seen at the gap. With increasing gap, plasma plume at the gap became larger. Laser beam penetrated the upper plate and irradiated the lower plate, and then a second molten pool on the lower plate was formed. More molten metal flowed towards the gap zone, and lower

and upper plates were joined together. For the T-joints with a gap size of 0.2 mm, 0.6 mm, 1.0 mm, the time from penetration to the uniting of the two separate molten pools was 8 ms, 22 ms, and 32 ms, respectively. After that, a keyhole was maintained in the state that occurred when the recoil force of the plasma evaporation balanced with the surface tension and the hydrostatic pressure. It was clear that the keyhole could maintain a quasi-stationary state when there was enough molten metal around the laser beam at the gap. As the gap increases, the formation of quasi-steady keyhole required more molten metal and longer time.

Figure 4 shows the dynamics of the molten pool and keyhole opening during CO₂ laser spot welding in different gap sizes. As shown in Fig. 4, after about 3 ms the pool surface was depressed by the intense evaporation of metal and the keyhole opening was clearly seen. The keyhole opening fluctuated less at zero gap, and its size became larger with increasing time. However, the largest size of keyhole opening with the gap appeared at 21.7 ms when the laser beam just penetrated the upper plate. At about 44.3 ms, the keyhole opening became dark as shown in Fig. 4 with a 0.6-mm or 1.0-mm gap. At this time, the laser beam completely penetrated the upper plate, and a part of plume in the keyhole escaped from the gap. The escaped plasma would increase with increasing gap, while the upper plasma decreased, leading to a darker keyhole opening.

The molten pool became larger and larger with increasing laser irradiation time. When the gap was zero, the size of

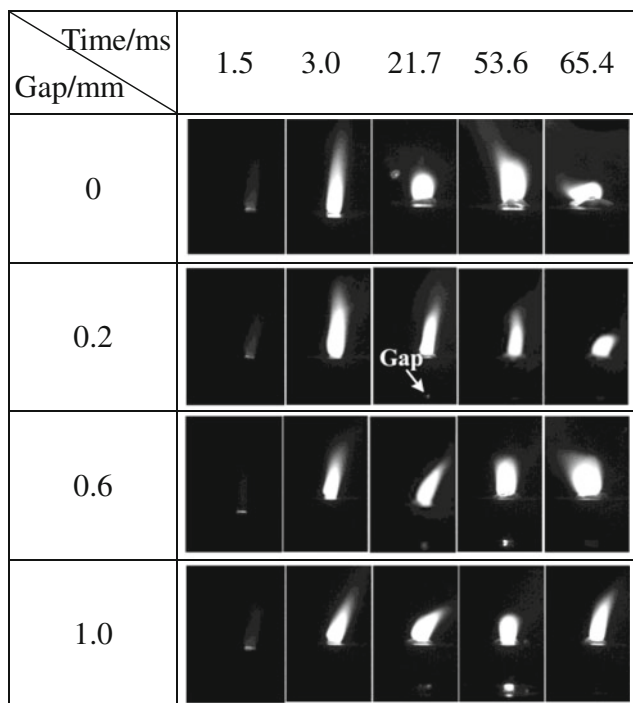


Fig. 3 Flaming images of laser-induced plume during laser spot welding in different gap sizes ($P=8$ kW, $nf=1,000$ f/s, He shield)

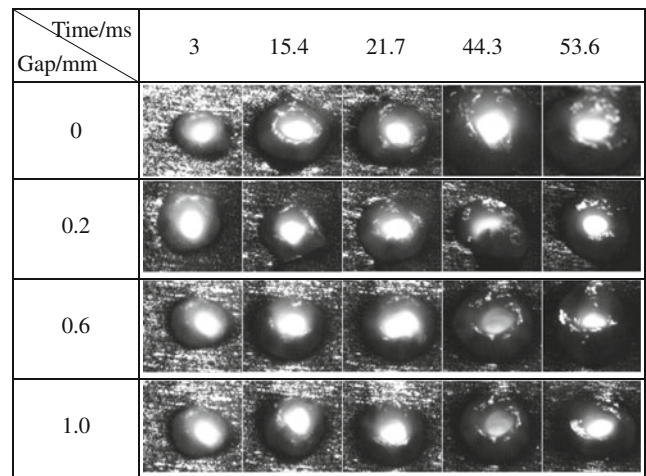


Fig. 4 Images of molten pool and keyhole opening in laser spot welding in different gap sizes ($P=8$ kW, $nf=750$ f/s, He shield)

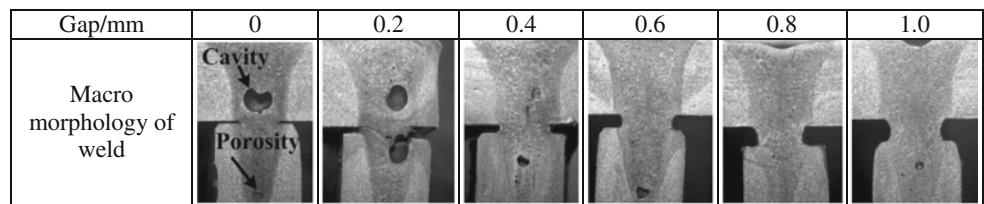
molten pool from 1.8 ms to 44.3 ms increased gradually and then became steady. The time became longer with increasing gap. The formation time of steady molten pool required 50.5 ms when the gap was 0.6 mm. The recoil pressure was smaller due to the plasma in the keyhole that decreased before the separate molten pool united, while after the separate molten pool united, a single keyhole formed again, and the penetration further increased. As stated above, the keyhole was no longer quasi-stationary sustained but fluctuates when a gap existed. Periodic decay and increase of energy in the keyhole completely coincided with the change of plume in different gap sizes as shown previously in Fig. 3.

Figure 5 is the macro morphology of overlap T-joint in laser spot welding in different gap sizes. As shown in Fig. 5, the porosities in T-joint reduced upon increasing the gap. When the gap was 0–0.4 mm, a large cavity was usually formed near the gap. In laser spot welding T-joints, shielding gas and metallic vapor were easily trapped in the keyhole because of the instability of the keyhole, when the gap was small, resulting in large cavities [13]. But when the gap was above 0.4 mm, only few pores appeared at the root of weld seam. The reason was that it was easier for metallic vapor to escape from the gap when gap was large. Therefore, in laser lap spot welding, appropriate gap helped to prevent porosity formation, but overlarge gap would cause depression of weld seam. As shown in Fig. 5, when gap was about 0.6 mm, weld defects were least.

3.2 Dynamics of molten pool and plume in laser continuous welding in different gap sizes

The dynamics of the plume were observed by high-speed cameras in the horizontal plane in laser continuous welding. Figure 6 shows the flaming images of the laser-induced plume in different gap sizes. As shown in Fig. 6, the size

Fig. 5 Macro morphology of overlap T-joint in laser spot welding in different gap sizes



and shape of plume fluctuated periodically when the gap was zero; fluctuation period was about 5.15 ms. Tilt angle of plume was almost perpendicular to the surface of the upper plate. As the gap increased gradually, plasma plume included three main dynamical characteristics. First, with increasing gap, the upper plume made the transition from cylinder to sphere, and its size became smaller. When front keyhole wall was disrupted at the gap, part of the plasma plume escaped, which led to variation of plasma plume distribution. Second, it was confirmed that the upper plume changed its evolution direction synchronized when the keyhole front wall was disrupted, which could not be kept straight and upright. Furthermore, the disruption time of keyhole front wall at the gap gradually increased with increasing gap. When the gap was 1 mm, front keyhole wall could not maintain well, and the plume escaped out at the gap frequently. As shown in Fig. 6, the existed time of plume at the gap was longer with increasing gap.

Figure 7 represents the change of keyhole opening and the motion of molten pool in CO₂ laser welding in different gap sizes. As shown in Fig. 7, a white round shape close to molten pool front was keyhole opening, and the verge of keyhole opening could be clearly seen. When the gap size

was zero, the size and shape of keyhole opening periodically fluctuated with the liquid surface of molten metal; the fluctuation cycle was about 6.2 ms. As the gap increased, keyhole opening fluctuated more violently, and the cycle of fluctuation got shorter. The molten pool and keyhole became more unstable with increasing gap, and may result in the powerful convection of molten pool. Because of the strong convection, a quick circulation of liquid was observed on the molten pool surface. The circulation period was about 5.2 ms and 3.9 ms when the gap was 0.2 mm and 0.6 mm, respectively. A lot of molten metal flowed to the gap after the laser penetrated the upper plate, which caused molten pool depression. Keyhole opening was not horizontally parallel to the liquid surface of molten pool, and the rear border of keyhole opening was the lowest point in the whole molten pool. As stated above, dynamics of molten pool and keyhole opening coincided well with the change of laser plume as shown previously in Fig. 6.

As shown in Fig. 7, the periodical fluctuation of molten pool was very obvious when the gap was zero, which was closely related to the instability of keyhole and plasma. A swelling near the keyhole opening also appeared, and molten metal flowed along the sides of the pool. With increasing gap, the wave was not eminent when molten pool appeared to depress. Molten metal near keyhole wall directly flowed backward from the middle of the pool and not along the sides; the upper keyhole could maintain stability [7]. The front wall of the keyhole at the gap became thinner and then disrupted under laser beam irradiation. The keyhole front wall closed again when the molten metal flowed to the gap. However, the front keyhole wall at the gap disrupted periodically, which destroyed the stationary state of the keyhole, and factors that resulted in the instability of the keyhole could cause the formation of porosities [14].

Figure 8 shows the dynamic images of laser-induced plume when the gap is 1.2 mm. As shown in Fig. 8, the laser beam penetrated the upper plate to lower plate, and the lower plume formed. With increasing radiation time, more plasma was ejected upward from the lower plate; thus, the upper and lower plume was held together. When more plasma was formed, reflection and absorption of plume maintained a major role, and lower plume disappeared. Because of a large gap, molten metal at the gap had solidified before joining together, so the upper and lower plate could not get united by the melt. According to previous works, keyhole was tilted in laser deep penetration welding [15, 16], and upper and lower

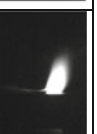
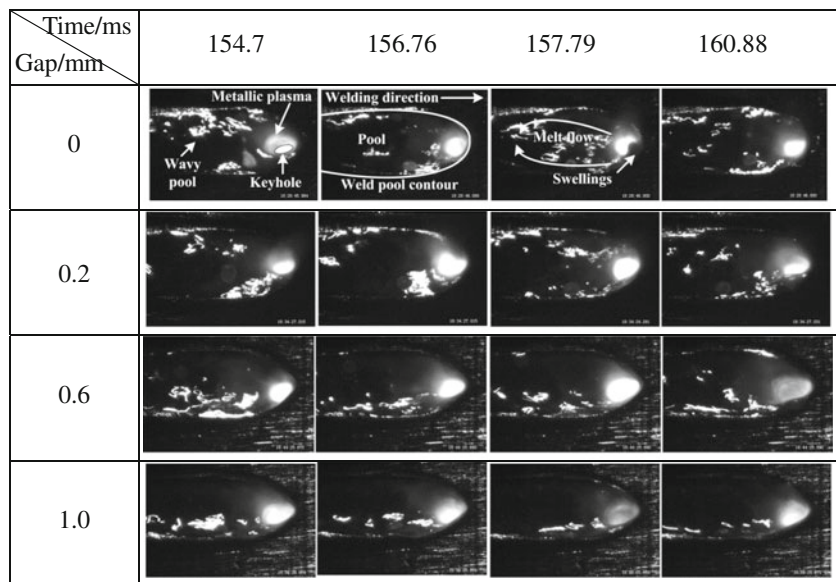
Time/ms Gap/mm	154.7	155.7	157.8	159.9	160.9
	0				
0.2					
0.6					
1.0					

Fig. 6 Images of laser-induced plume in laser continuous welding in different gap sizes ($P=8$ kW, $v=1.5$ m/min, $nf=1,000$ f/s, He shield)

Fig. 7 Dynamics of keyhole opening and molten pool in laser continuous welding in different gap sizes ($P=8$ kW, $v=1.5$ m/min, $nf=750$ f/s, He shield)



plume was not in a vertical line. As stated above, we could also infer that the union of the separate melt pool at the gap was the combined effects of the upper and lower plume and molten pool.

With increasing gap, the dynamics of the plume coincided well with keyhole and molten pool. Beam energy was not uniformly absorbed on the keyhole wall, while the evaporation intensity also changed cyclically, and, hence, keyhole as well as the molten pool was disturbed by the strong vapor jet. Keyhole was no longer quasi-stationary sustained but fluctuates with increasing gap. Periodic closure and disruption of front keyhole wall enhanced welding process instability in different gap sizes, which was closely related to the porosity formation.

3.3 Porosity formation process analysis and suppression methods in laser continuous welding

Figure 9 shows the macro morphology of the overlap T-joint in different gap sizes. As shown in Fig. 9, distribution of

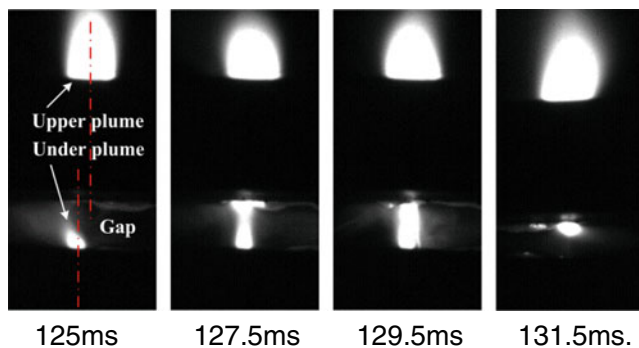


Fig. 8 Dynamic images of laser-induced plume when the gap is 1.2 mm ($P=8$ kW, $v=1.5$ m/min, $nf=850$ f/s)

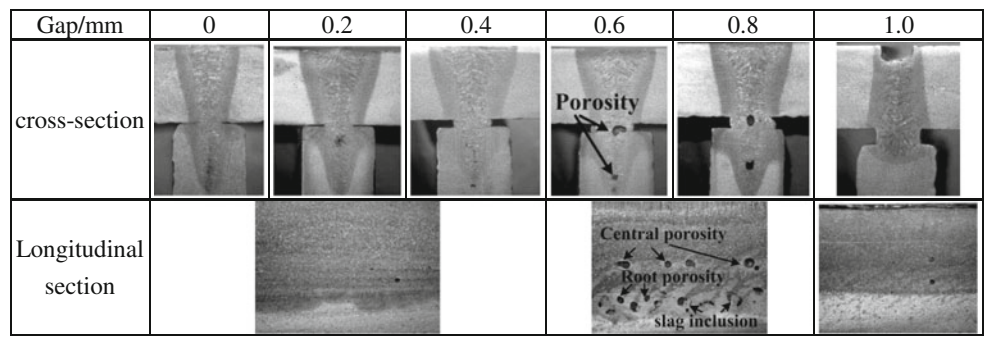
porosity was different from laser spot welding with increasing gap. When the gap was less than 0.4 mm, porosities were less in laser continuous welding. When the gap was 0.4–0.8 mm, plenty of porosities appeared at the gap and root of weld seam. When the gap was 1.0 mm, porosities were less, while the morphology of the weld occurred to change and depression was very obvious.

The above-stated optical observations revealed that gap caused keyhole instability periodically, which was closely related to the porosity formation. Therefore, the instability of keyhole was the main reason of porosity formation, which was closely related to the dynamics of plume and molten pool. When the gap was less than 0.8 mm, macrograph of cross-sections of the weld seams showed well-known “wine cup shape” characteristics [17]. When the gap was above 0.8 mm, the weld seam presents reverse “wine cup shape”. The plume could easily escape from the gap when the gap was large, which led to a change of weld seam.

As previously mentioned, in laser overlap welded T-joints, there were two kinds of porosities that distributed at the root and the gap, respectively. The formation mechanisms of both porosities were different. The formation cause of root porosity was instability (fluctuations) of keyhole, especially when the gap was small. Because of the instability of the keyhole, metal vapor enters into the keyhole, resulting in root porosity, which also coincided with previous works [18]. The main formation cause of porosity in center was the periodical disruption and closure of front keyhole wall at the gap. The motion of molten pool occurred to vary. The bubbles were easily trapped in the gap. The distribution characteristics of porosity in different gaps had an excellent agreement with plume and molten pool dynamics.

In laser continuous welding, the formation and suppression of root porosity were extensively discussed by Seto [9].

Fig. 9 Macro morphology of overlap T-joint and the characteristic porosity in different gap sizes

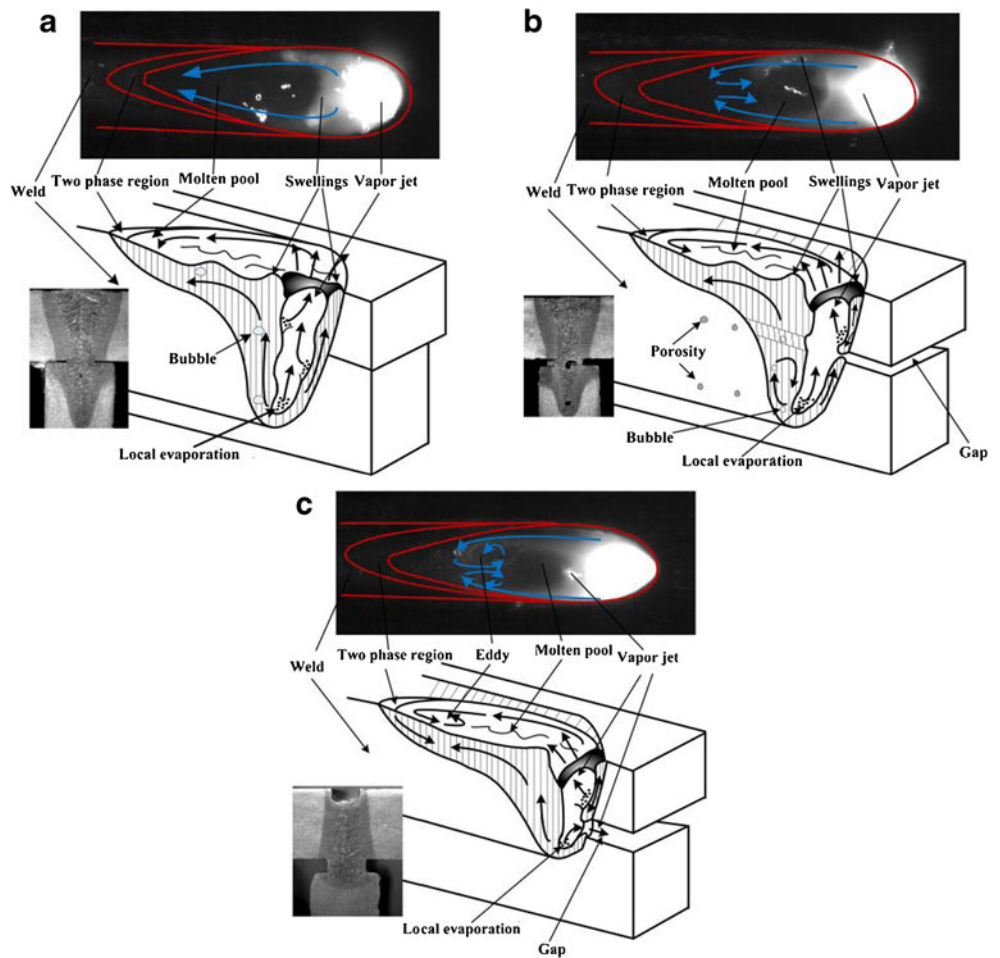


The controlled pulse modulation could effectively reduce the porosity formation by forced oscillations of the keyhole. Suppression methods of porosity were different in laser lap welding. Firstly, the essential point was to keep the gap under 0.4 mm and maintain the condition at a quasi-stationary state, which required the plates above and below to fit well together. Secondly, low welding velocity was very effective to reduce or suppress the porosity formation. Under this condition, more molten pool flowed to the gap, and the quasi-stationary keyhole could easily be formed, which helped bubbles to escape from the molten pool.

4 Discussion

Some studies have been conducted on keyhole and molten pool dynamic behavior, while the influence of gap on dynamics of keyhole and molten pool is still vague in laser overlap welding. In this paper, in order to better understand and illustrate the effect of gap on keyhole and molten pool behavior in laser continuous welding, the authors built three simple models for keyhole behavior and molten pool motions. Figure 9 presents different regimes of the keyhole and molten pool in CO₂ laser welding in different gap sizes.

Fig. 10 Schematic of molten pool and keyhole in laser continuous welding in different gap sizes. **a** 0–0.4 mm, **b** 0.4–0.8 mm, **c** 0.8–1.0 mm



According to the analysis above, the dynamic behavior of molten pool and keyhole can be divided into three different regimes that are quasi-stationary regime, non-stationary regime, and false-stationary regime, and the corresponding gap is 0–0.4 mm, 0.4–0.8 mm, and 0.8–1.0 mm, respectively.

The first regime (Fig. 10a), which is observed when the gap is less than 0.4 mm, is characterized by quasi-stable keyhole and molten pool motion. Under this state, molten pool surface shows chaotic fluctuations and large swellings of liquids fluctuating around the keyhole aperture, and a laminar flow cannot be observed around the keyhole [19]. There is no obvious return flow in the rear of molten pool, and internal pressure inside the keyhole, generated by the ejected metallic vapor from the keyhole wall, is not large enough for counterbalancing the closing pressure of the keyhole due to surface tension effects [20]. Because of a single molten pool induced by a small gap, the bubbles formed by instable keyhole could easily escape from the molten pool. When the gap is larger than 0.8 mm, turbulence and eddies remarkably appear during laser welding. The plume in the keyhole continuously jets out at the gap. The keyhole is “quasi-stationary” sustained. In this regime, the keyhole becomes shallower when a large amount of plume continuously escapes at the gap. The bubbles induced by instability of keyhole are less, and porosities were difficult to form (Fig. 9).

When the gap is 0.4–0.8 mm, molten metal of upper and lower plate accumulates at the gap, and a single keyhole forms. Because of surface tension, the keyhole front wall becomes thinner until it is disrupted at the gap. Plume and metal vapor in keyhole spurt from the gap. Then the front keyhole wall tends to unite again. In this regime, the keyhole cannot maintain stability and exhibited a non-stationary regime. The local disruption of the front keyhole wall at the gap changes balance between surface tension and hydrostatic pressure, and the motion of molten pool also changes. In penetration laser welding, keyhole instability has been considered to be the main reason of bubble initiation. Porosities resulted from bubbles trapped when the weld pool solidifies [21]. As shown in Fig. 10c, at first, periodical disruption and closure of front keyhole wall aggravated the instability of the keyhole. Second, the gap changes the molten pool motion when the gap is 0.4–0.8 mm. Plenty of bubbles produced at the bottom of keyhole cannot get through molten pool at the gap, which is trapped in molten pool in the gap, forming porosities at the gap [22].

Beam energy is not uniformly absorbed on the keyhole wall with increasing gap; keyhole as well as molten pool is easily disturbed by strong vapor jet. Hence, the keyhole is no longer quasi-stationary sustained but fluctuates with increasing gap, which causes the periodic closure and disruption of front keyhole wall, and it is closely related to the porosity formation. The change coincided well with the analysis

above for dynamics, and we can better understand the formation mechanism of porosity.

5 Conclusion

The major conclusions obtained in this work are as follows:

1. The dynamics of plume and molten pool in laser spot welding and laser continuous welding of T-joint were observed by high-speed videos in different gap sizes. In laser spot welding, the time from penetrating the upper plate to formation of stable keyhole increased with increasing gap. In laser continuous welding, the plume had three main dynamical variations: size, inclination angle, and the existed time of gap plume, respectively. The dynamics of plume coincided well with molten pool and keyhole.
2. In laser continuous welding, the distribution of beam energy occurred to change on the keyhole wall with increasing gap. Keyhole was no longer quasi-stationary sustained but fluctuated with increasing gap, which caused the periodic closure and disruption of the front keyhole wall. Dynamics of plume and molten pool coincided well with the distribution characteristics of porosity in different gaps.
3. The formation mechanism of porosity in continuous welding was different from laser spot welding. In laser continuous welding, molten pool motion and stability of keyhole occurred to vary for the gap. Bubbles were easily trapped in the molten pool in the gap, and porosities formed at the gap and root of weld seam. In laser spot welding, a large gap was conducive to escape of gas in the keyhole, thus the porosities were less.
4. In laser continuous welding, a method to reduce or suppress porosity in laser lap welding was to control gap less than 0.4 mm. In laser lap spot welding, a large gap could help prevent the formation of porosity.

Acknowledgment This work was supported by the National Natural Science Foundation of China (grant no. 51035004)

References

1. Romanoff J, Remes H, Jutila M (2007) The stiffness of laser stake welded T-joints in web-core sandwich structures. *Thin-Walled Struct* 45(4):453–462
2. Yoon SH, Hwang JR, Na SJ (2007) A study on the plasma-augmented laser welding for small-diameter STS tubes. *Int J Adv Manuf Technol* 32:1134–1143
3. Ho CY, Wen MY (2004) Distribution of the intensity absorbed by the keyhole wall in laser processing. *J Mater Process Technol* 145:303–310

4. Anhua L, Xinhua T, Fenggui L (2013) Arc profile characteristics of Al alloy in double-pulsed GMAW. *Int J Adv Manuf Technol* 65:1–7
5. Zhiguo G, Yixiong W, Huang J (2009) Analysis of weld pool dynamic during stationary laser–MIG hybrid welding. *Int J Adv Manuf Technol* 44:870–879
6. Poueyo-Verwaerde A, Fabbro R, Deshors G (1993) Experimental study of laser-induced plasma in welding conditions with continuous CO₂ laser. *J Appl Phys* 74:5773–5780
7. Szymanski Z, Kurzyna J (1994) Spectroscopic measurements of laser induced plasma during welding with CO₂ laser. *J Appl Phys* 76:7750–7756
8. Matsunawa A, Kim JD, Seto N (1998) Dynamics of keyhole and molten pool in laser welding. *J Laser Appl* 10:247–254
9. Seto KS, Matsunawa A (2000) High-speed simultaneous observation of plasma and keyhole behavior during high power CO₂ laser welding: effect of shielding gas on porosity formation. *J Laser Appl* 6:245–250
10. Guohua L, Yan C, Yixiong W (2009) Stability information in plasma image of high-power CO₂ laser welding. *Opt Lasers Eng* 47:990–994
11. Kroos J, Gratzke U, Vicaneck M, Simon G (1993) Dynamic behaviour of the keyhole in laser welding. *J Phys D Appl Phys* 26:481–486
12. Fabbro R, Hamadou M, Coste F (2004) Metallic vapor ejection effect on melt pool dynamics in deep penetration laser welding. *J Laser Appl* 16(1):16–19
13. Kaplan A (1994) A model of deep penetration laser welding based on calculation of the keyhole profile. *J Phys D Appl Phys* 27:1805–1814
14. Kaplan AFH, Mizutani M, Katayama S, Matsunawa A (2002) Unbounded keyhole collapse and bubble formation during pulsed laser interaction with liquid zinc. *J Phys D Appl Phys* 35:1218–1228
15. Fujinaga S, Takenaka H, Narikiyo T (2000) Direct observation of keyhole behaviour during pulse modulated high-power Nd:YAG laser irradiation. *J Phys D Appl Phys* 33:492–497
16. Xiangzhong J, Lijun L, Yi Z (2004) A heat transfer model for deep penetration laser welding based on an actual keyhole. *Int J Heat Mass Transf* 46:15–22
17. Changa WS, Nab SJ (2002) A study on the prediction of the laser weld shape with varying heat source equations and the thermal distortion of a small structure in micro-joining. *J Mater Process Technol* 120:208–214
18. Matsunawa A, Katayama S, Kohsaka S (1993) Pulse shape optimization for defect prevention in pulsed laser welding of stainless steel. *ICALEO Proceedings* 77:487–497
19. Momin O, Shuja SZ (2012) CO₂ laser heating of surfaces: melt pool formation at surface. *Opt Laser Technol* 44(2):463–470
20. Dowden J (2002) Interaction of the keyhole and weld pool in laser keyhole welding. *J Laser Appl* 14:204–209
21. Tsukamoto S (2011) High speed imaging technique part 2—high speed imaging of power beam welding phenomena. *Sci Technol Weld Join* 16:44–55
22. Peter B, Helmut H, Thomas G (2011) Understanding pore formation in laser beam welding. *Physics Procedia* 12:241–247